



Cold cloud microphysical process rates in a global chemistry-climate model

Sara Bacer^{1,*}, Sylvia C. Sullivan², Holger Tost³, Jos Lelieveld^{1,4}, and Andrea Pozzer^{1,5}

¹Atmospheric Chemistry Department, Max Planck Institute for Chemistry, Mainz, Germany

²Institute of Meteorology and Climate Research, Karlsruhe Institute of Technology, Karlsruhe, Germany

³Institute for Atmospheric Physics, Johannes Gutenberg University Mainz, Mainz, Germany

⁴Energy, Environment and Water Research Center, The Cyprus Institute, Nicosia, Cyprus

⁵International Centre for Theoretical Physics, Trieste, Italy

**now at:* LEGI, Université Grenoble Alpes, CNRS, Grenoble INP, Grenoble, France

Correspondence: Sara Bacer (sara.bacer@univ-grenoble-alpes.fr)

Abstract. Microphysical processes in cold clouds which act as sources or sinks of hydrometeors below 0°C control the ice crystal number concentrations (ICNCs) and in turn the cloud radiative effects. Estimating the relative importance of the cold cloud microphysical process rates is of fundamental importance to underpin the development of cloud parameterizations for weather, atmospheric chemistry and climate models and compare the output with observations at different temporal resolutions.

5 This study quantifies and investigates the cold cloud microphysical process rates by means of the chemistry-climate model EMAC and defines the hierarchy of sources and sinks of ice crystals. The analysis is carried out both at global and at regional scales. We found that globally the freezing of cloud droplets, along with convective detrainment over tropical land masses, are the dominant sources of ice crystals, while aggregation and accretion act as the largest sinks. In general, all processes are characterised by highly skewed distribution. Moreover, the influence of (a) different ice nucleation parameterizations and
10 (b) a future global warming scenario on the rates has been analysed in two sensitivity studies. In the first, we found that the application of different parameterizations for ice nucleation changed only slightly the hierarchy of ice crystal sources. In the second, all microphysical processes followed an upward shift (in altitude) and an increase by up to 10% in the upper troposphere towards the end of the 21st century. This increase could have important feedbacks, such as leading to enhanced longwave warming of the uppermost atmosphere.

15 1 Introduction

Clouds play a central role in the global energy budget interacting with shortwave solar and longwave terrestrial radiation. Their radiative properties (cloud albedo and emissivity) depend on microphysical and optical characteristics, such as temperature, size distribution and shape of cloud particles, and the phase of water. Despite the great relevance in the Earth System, the understanding of clouds is still challenging and affected by large uncertainties (IPCC, 2013). The numerical representation
20 of clouds must contend with the limited understanding of the fundamental details of microphysical processes as well as the fact that cloud processes span several order of magnitudes (from nanometres to thousands of kilometres). Hence, modelling of



clouds remains a weak point in all atmospheric models, regardless of their resolution, and has been recognised as one of the dominant sources of uncertainty in climate studies (IPCC, 2013; Seinfeld et al., 2016).

Modelling the microphysics of cold clouds, which form at temperatures lower than 0°C and involve ice crystals (ICs), is more challenging than that of warm clouds because of the additional complexity of ice processes (Cantrell and Heymsfield, 2005; Kanji et al., 2017; Heymsfield et al., 2017; Korolev et al., 2017). Some examples of these processes are heterogeneous ice nucleation, which depends on particular aerosols and occurs via different modes, the secondary production mechanisms of ice crystals, which involve collisions of ICs, the competition for water vapour among different ice particles, and the thermodynamic instabilities when both liquid and ice phases coexist. Additionally, the variety of possible ice crystal shapes from dendrites to needles also determines the radiative impact of cold clouds and complicates their representation in large-scale models (Lawson et al., 2019). Cold clouds are classified as cirrus clouds, when they purely consist of ICs at temperatures generally lower than -35°C , and mixed-phase clouds, when they include both ICs and supercooled liquid cloud droplets between -35°C and 0°C . Cirrus clouds strongly impact the transport of water vapour entering the stratosphere, which in turn has a strong effect on radiation and ozone chemistry (Jensen et al., 2013), and produce a positive net radiative effect at the top of the atmosphere (TOA) (Chen et al., 2000; Hong et al., 2016; Matus and L'Ecuyer, 2017); on the other hand, mixed-phase clouds exert a negative net radiative effect at the TOA, although the estimates of their radiative effect are complicated by the coexistence of both ice and liquid cloud phases (Chen et al., 2000; Hong et al., 2016; Matus and L'Ecuyer, 2017).

Several microphysical processes have been identified in cold clouds (Pruppacher and Klett, 1997) that can be broadly classified as formation, growth, and loss processes of ice crystals. New ICs are formed thermodynamically via two ice nucleation mechanisms, depending on environmental conditions (e.g. temperature, supersaturation, and vertical air motions) and aerosol populations (i.e. aerosol number concentrations and physicochemical characteristics, such as composition, shape, and surface tension) (Pruppacher and Klett, 1997; Kanji et al., 2017; Heymsfield et al., 2017). Homogeneous ice nucleation occurs at low temperatures (below -35°C) and high ice saturation ratios ($140\% - 160\%$) via the freezing of supercooled liquid cloud droplets. Heterogeneous ice nucleation takes place at warmer but still subzero temperatures and lower ice supersaturation thanks to the presence of particular atmospheric aerosols, called ice nucleating particles (INPs). It occurs via four different mechanisms, or ice nucleation modes: contact nucleation, condensation nucleation, immersion, and deposition nucleation modes. ICs can also be produced from the multiplication of pre-existing ice crystals, via the so-called secondary ice production (or ice multiplication). Several mechanisms of secondary ice production have been identified. In rime splintering (or the Hallett-Mossop process), small ice crystals (or splinters) are ejected after the capture of supercooled droplets by large ice particles (e.g. graupels) between -3°C and -8°C . In collisional break-up (or collisional fragmentation), the disintegration of fragile, slower-falling dendritic crystals which collide with dense graupel particles produces smaller ice particles. Droplet shattering involves the freezing of large cloud droplets and their subsequent shattering. Sublimation fragmentation occurs when ice particles break from parent ice particles after the sublimation of "ice bridges" at ice subsaturated conditions. Additionally, ICs can be generated in the vicinity of deep convective clouds by their lateral outflow or detrainment.

A variety of ice growth mechanisms also exist. In conditions of ice supersaturation, ICs grow by diffusion as ambient water vapour deposits. When both ice and liquid phases coexist, the water vapour is generated by evaporating water droplets because



of the difference between the saturation vapour pressure over ice and over water (Wegener-Bergeron-Findeisen – WBF mechanism). The collision-coalescence (or collection) between ICs and other hydrometeors is another growth mechanism which occurs in several ways (Rogers and Yau, 1989; Khain and Pinsky, 2018): self-collection consists of the collision-coalescence
60 between ICs and the production of ice crystals with larger size; aggregation occurs when the colliding ICs clump together to form an aggregated snowflake; accretion indicates the collection between ice crystals and snowflakes; and riming refers to the collision of ICs with supercooled liquid droplets which freeze upon contact. Melting and sublimation are other sinks of ice crystals when temperatures are higher than 0°C and there is ice subsaturation, respectively.

Ice water content, the particle size distribution, and cloud optical depth all depend on ice crystal number concentration
65 (ICNC), and their improved representation in models allows for more realistic estimates of the cloud radiative effects. For this reason, many efforts have been made to parameterize all relevant microphysical processes which affect ICNC (e.g. Kärcher and Lohmann, 2002a; Barahona and Nenes, 2008; Phillips et al., 2007; DeMott et al., 2010; Hallett and Mossop, 1974) and to further improve the existing parameterizations (e.g. Kärcher and Lohmann, 2002b; Barahona and Nenes, 2009; Phillips et al., 2013; DeMott et al., 2016; Sullivan et al., 2018b, a). The parameterizations have been implemented in general circulation
70 models (GCMs) which may use a two-moment cloud microphysics scheme (e.g. Liu et al., 2012; Barahona et al., 2014; Kuebbeler et al., 2014; Bacer et al., 2018) to advance the simulation of cloud phase partitioning and cloud-radiation feedbacks.

It is of crucial importance to know the hierarchy of sources and sinks of ICs under different thermodynamic conditions and over different time scales. In fact, knowing these relative contributions facilitates the comparison of simulation output with observations across temporal resolutions and the development of scale-aware microphysics schemes. Gettelman et al. (2013)
75 analysed the rates of the processes affecting precipitation (e.g. condensation, accretion, autoconversion, sedimentation of liquid droplets, WBF, homogeneous nucleation, and heterogeneous nucleation) in the CAM5 model. To the best of our knowledge, a quantitative analysis of all the microphysical processes affecting ICNC has not yet been performed. Therefore, this study aims to estimate and investigate the rates of the microphysical processes which act as sources or sinks of ice crystals and control ICNC in cold clouds for the first time. The analysis is carried out both at global and at regional scales. We also discuss how
80 the rates will change under a global warming scenario towards the end of the century. For this study, the numerical simulations have been performed with the global ECHAM/MESSy Atmospheric Chemistry (EMAC) model.

The paper is organised as follows. We first describe the EMAC model and the numerical representation of the ice microphysical processes inside the model (Section 2). Then, the simulations are detailed (Section 3) and model output at both the global and the regional scale is presented (Section 4). We also show the robustness of these results to the ice nucleation
85 parameterization, as well as their sensitivity to global warming with an RCP6.0 simulation. We finish with our Conclusions.

2 Ice microphysical processes in EMAC

2.1 The EMAC model

The EMAC model is a global chemistry-climate model which describes tropospheric and middle-atmospheric processes and their interactions with ocean, land, and human influences. EMAC combines the 5th generation European Centre Hamburg GCM



90 (ECHAM5, Roeckner et al., 2006), the core of the atmospheric dynamics computations, with the Modular Earth Submodel System (MESSy, Jöckel et al., 2010), which includes a variety of submodels describing physical, dynamical, and chemical processes. For the present study we used ECHAM5 version 5.3.02 and MESSy version 2.53.

The EMAC model has been extensively used and evaluated against in-situ, aircraft, and satellite observations of, for example, aerosol optical depth, acid deposition, meteorological parameters, cloud radiative effects (e.g. Pozzer et al., 2012, 2015; Karydis
95 et al., 2016; Tsimpidi et al., 2016; Klingmüller et al., 2018; Bacer et al., 2018). EMAC computes gas-phase species online through the Module Efficiently Calculating the Chemistry of the Atmosphere (MECCA) submodel (Sander et al., 2011) and provides a comprehensive treatment of chemical processes and dynamical feedbacks through radiation (Dietmüller et al., 2016). Aerosol microphysics and gas/aerosol partitioning are calculated by the Global Modal-aerosol eXtension (GMXe) submodel (Pringle et al., 2010), a two-moment aerosol module which predicts the number concentration and the mass mixing
100 ratio of the aerosol modes. The aerosol size distribution is described by seven lognormal modes: four hydrophilic modes, which cover the aerosol size spectrum of nucleation, Aitken, accumulation, and coarse particles, and three hydrophobic modes, which have the same size range except for the nucleation particles. The aerosol composition within each mode is uniform (internally mixed) but it varies among the modes (externally mixed). The ONEMIS and OFFEMIS submodels describe the online and offline emissions, respectively, of tracers and aerosols, while the TNUDGE submodel performs the tracer nudging
105 towards observations (Kerkweg et al., 2006b). Physical loss processes, like dry deposition, wet deposition, and sedimentation of aerosols and trace gases, are explicitly considered by the submodels DDEP, SEDI, and SCAV (Kerkweg et al., 2006a; Tost et al., 2006a). The RAD submodel (Dietmüller et al., 2016) calculates the radiative transfer taking into account cloud cover, optical properties of clouds and aerosols, mixing ratios of water vapour and radiatively active species, and orbital parameters. Convective and large-scale clouds are parameterized via two different submodels, the CONVECT submodel (Tost et al., 2006b)
110 and the CLOUD submodel (Roeckner et al., 2004), as described in the next Subsection.

In EMAC, a single updraft velocity (w) is used for the whole grid cell, although the vertical velocity varies strongly in reality within the dimensions of a grid box (e.g. Guo et al., 2008). This is a simplification which is commonly used by GCMs. The subgrid-scale variability of vertical velocity (w_{sub}) is introduced by a turbulent component which depends on the subgrid-scale turbulent kinetic energy (TKE) described by Brinkop and Roeckner (1995). Thus, the vertical velocity is given by the sum of
115 the grid mean vertical velocity (\bar{w}) and the turbulent contribution: $w = \bar{w} + 0.7\sqrt{TKE}$ (Lohmann and Kärcher, 2002).

2.2 Numerical representation of clouds

Convective cloud microphysics in EMAC is solely based on temperature and updraft strength and does not take into account the aerosol influence on cloud droplet and ice crystal formation. To simulate convective clouds, the CONVECT submodel includes multiple parameterizations which address the influence of the convective activity on the larger scale circulation. The
120 detrained water vapour is added to the large-scale water vapour field. The detrained cloud condensate is used as a source term for the cloud condensate treated by the CLOUD submodel and it is considered in the liquid or ice phase depending on its temperature (if the temperature is lower than -35°C the phase is ice, otherwise it is liquid). In this work, the scheme of Tiedtke (1989) with modifications by Nordeng (1994) has been used.



The CLOUD submodel describes physical and microphysical processes in large-scale stratiform clouds. It uses a double-
125 moment cloud microphysics scheme for cloud droplets and ice crystals (Lohmann et al., 1999; Lohmann and Kärcher, 2002;
Lohmann et al., 2007) and solves the prognostic equations for specific humidity, liquid cloud mixing ratio, ice cloud mixing
ratio, cloud droplet number concentration (CDNC), and ICNC. Cloud droplet formation is computed by an advanced physically
based parameterization (Kumar et al., 2011; Karydis et al., 2011) which merges two theories: the κ -Köhler theory (Petters and
Kreidenweis, 2007), which governs the activation of soluble aerosols, and the Frenkel-Halsey-Hill adsorption activation theory
130 (Kumar et al., 2009), which describes the droplet activation due to water adsorption onto insoluble aerosols (e.g. mineral dust).
This parameterisation is applied to the aerosols that consist of an insoluble core with soluble coating, while soluble aerosols
follow the κ -Köhler theory (Karydis et al., 2017). In the cirrus regime, the ice crystals can form either via homogeneous nucle-
ation, using the parameterization of Kärcher and Lohmann (2002b, KL02), or via homogeneous and heterogeneous nucleation
using the parameterization of Barahona and Nenes (2009, BN09), which takes into account the competition for the available
135 water vapour between the two ice nucleation mechanisms and among the pre-existing ice crystals (Bacer et al., 2018). In the
mixed-phase regime, contact nucleation is simulated according to Lohmann and Diehl (2006, LD06). Immersion nucleation
can be parameterized via LD06 or via the empirical parameterization of Phillips et al. (2013, P13), which can also simulate de-
position nucleation. Cloud cover is computed diagnostically with the scheme of Sundqvist et al. (1989), based on the grid-mean
relative humidity. Other microphysical processes, like phase transitions, autoconversion, aggregation, accretion, evaporation of
140 rain, melting of snow, sedimentation of cloud ice, are also taken into account by the CLOUD submodel.

2.3 Ice microphysical processes

According to Lohmann (2002) and Roeckner et al. (2004), the evolution of ICNC (i.e. rate or *tendency* of ICNC) is described
by the following prognostic equation:

$$\frac{\partial \text{ICNC}}{\partial t} = R_{transp} + R_{sedi} + R_{ncir} + R_{nmix} + R_{secp} - (R_{self} + R_{aggr} + R_{accr} + R_{melt} + R_{subl}) \quad (1)$$

145 where the R -terms (in $\text{m}^{-3}\text{s}^{-1}$) are the ICNC tendencies due to specific (micro)physical processes: advective, turbulent,
and convective transport (R_{transp}), sedimentation (R_{sedi}), ice nucleation in the cirrus regime (R_{ncir}), ice nucleation in the
mixed-phase regime (R_{nmix}), secondary ice production (R_{secp}), self-colletion (R_{self}), aggregation (R_{aggr}), accretion (R_{accr}),
melting (R_{melt}), and sublimation (R_{subl}) of ice crystals. Transport as well as sedimentation of ICs are computed for the grid-
box volume ($\overline{\text{ICNC}}$), while the other terms are in-cloud processes ($\text{ICNC}_{\text{in-cloud}}$). The latter ones are related to the grid-mean
150 values via the fractional cloud cover (f_C): $\text{ICNC}_{\text{in-cloud}} = \overline{\text{ICNC}}/f_C$. Among the processes in equation (1), advective, turbulent,
and convective transport and sedimentation (which is formally treated like vertical advection) are physical processes solved by
the model, while all others are microphysical processes computed with different parameterizations.

In this work, we decompose the microphysical sources and sinks of ICs in the CLOUD submodel (Table 1), i.e. all R -terms
except R_{transp} . (More information can be found in the cited works and references therein.)

155 **Sources of ice crystals.** The number of new ICs originating from convective detrainment (DETR) is estimated from the
detrained cloud condensate in the ice phase (i.e. when temperatures are lower than 35°C , see Subsection 2.2) by assuming a



temperature dependent radius. DETR is included in the transport term of equation (1) (Roeckner et al., 2004), but it will be studied here as an independent source of ICs defined within the CLOUD submodel. As described in Subsection 2.2, ice crystal formation in the cirrus regime (NCIR) is simulated by the ice nucleation parameterizations BN09 or KL02. The new ICs in the mixed-phase regime (NMIX) are the sum of the ice crystals originated from contact, immersion/condensation, and deposition nucleation modes, i.e. the results of the heterogeneous nucleation parameterizations LD06 and/or P13 applied in this regime. Secondary ice production (SECP) occurs via the Hallet-Mossop process between -3°C and -8°C as described in Levkov et al. (1992). Another source of ICs is the instantaneous freezing of supercooled cloud droplets (FREE): when temperatures are below -35°C , the cloud droplets which did not freeze through ice nucleation become ICs. FREE represents (in a numerical way) the so-called liquid-origin cirrus, i.e. cirrus clouds formed by ICs originated via homogeneous nucleation at temperatures near the homogeneous nucleation threshold which are then lifted in the cirrus regime. Instead, NCIR represents the in-situ cirrus, i.e. cirrus clouds which form directly at temperatures colder than -35°C (Krämer et al., 2016).

Sinks of ice crystals. Self-collection (SELF), aggregation (AGGR), and accretion (ACCR) of ice crystals follow Lin et al. (1983) and Levkov et al. (1992). It is assumed that ice crystals melt as soon as temperatures are above 0°C (MELT).

Sources and sinks of ice crystals. Sedimentation (SEDI) is a physical process which impacts ICNC by vertically redistributing the ice crystals. Although it does not really produce or remove ICs, it can be considered as source or sink relative to a selected region or period. SEDI includes also the sublimation of falling ICs which encounter an ice subsaturated region.

It is important to mention that the CLOUD submodel includes also some ICNC tendencies which are defined only with the aim of assuring the physical realism of some processes or parameterizations (e.g. the ICNC value must be smaller than the maximal threshold of 10^7 m^{-3} at each model integration time). However, since these “numerical tendencies” do not have their own physical meaning, they are not considered in this work.

3 Setup of simulations

The simulations in this study have been performed at T42L31ECMWF resolution, which corresponds to a spherical truncation of T42 (i.e. quadratic Gaussian grid of approximately $2.8^{\circ} \times 2.8^{\circ}$, in latitude and longitude) and 31 vertical hybrid pressure levels up to 10 hPa (about 25 km). The model time step is 20 minutes, and the model results are stored with a frequency of 5 hours. The simulations are 2 years long: the first year has been considered spin-up time, while the second year has been used for the analysis. Two periods are taken into account: the years 2000-2001 to represent present-day conditions and the years 2080-2081 to represent a future period. The simulations are forced by prescribed sea surface temperatures (SSTs) and sea-ice concentrations (SICs). SSTs and SICs are provided by the Hadley Centre Global Environment Model version 2 – Earth System (HadGEM2-ES) Model (Collins et al., 2011): the historical simulation with HadGEM2-ES is used for the present period, while the RCP6.0 simulation is considered for the future (like in the simulation RC2-oce-01 of the ESCiMo project described in Jöckel et al., 2016). Aerosols are emitted offline using monthly emission files based on the AEROCOM data set, such as for mineral dust, secondary organic aerosol, and sea salt (like in Pozzer et al., 2012), or a combination of the ACCMIP (Lamarque



Tendency	Description	Temperature
<i>Sources of ice crystals</i>		
DETR	Convective detrainment	$T < -35^{\circ}\text{C}$
NCIR	Ice nucleation in the cirrus regime	$T < -35^{\circ}\text{C}$
FREE	Instantaneous freezing	$T < -35^{\circ}\text{C}$
NMIX	Ice nucleation in the mixed-phase regime	$-35^{\circ}\text{C} < T < 0^{\circ}\text{C}$
SECP	Secondary ice production	$-8^{\circ}\text{C} < T < -3^{\circ}\text{C}$
<i>Sinks of ice crystals</i>		
MELT	Melting	$T > 0^{\circ}\text{C}$
SELF	Self-collection	$T < 0^{\circ}\text{C}$
AGGR	Aggregation	$T < 0^{\circ}\text{C}$
ACCR	Accretion	$T < 0^{\circ}\text{C}$
<i>Sources and Sinks</i>		
SEDI	Sedimentation	$T < 0^{\circ}\text{C}$

Table 1. ICNC tendencies (or rates) defined in the CLOUD submodel. The first column contains the abbreviations associated with each tendency; the second column describes the (micro)physical processes associated with each tendency; the third column specifies the temperature range in which the processes occur.

Experiment name	Ice nucleation scheme	
	<i>Cirrus regime</i>	<i>Mixed-phase regime</i>
REF	BN09	P13
PRES	KL02	LD06
FUT	BN09	P13

Table 2. Simulations carried out and analysed in this study.

et al., 2010) and RCP 6.0 scenario (Fujino et al., 2006), such as for black carbon and organic carbon with biomass burning and anthropogenic origins.

The simulations carried out in this study are one reference run and two sensitivity case studies (Table 2). The reference run (REF) simulates recent conditions and applies the ice nucleation parameterizations BN09 and P13 in the cirrus regime and mixed-phase regime, respectively (like in Bacer et al., 2018). REF will be analysed in order to quantify the rates of ice (micro)physical processes in cold clouds and define their relative importance. Another simulation (PRES) which refers to the same period but uses different ice nucleation schemes has been performed to analyse the effects on the ICNC tendencies due to a different choice of parameterizations. In particular, the simulation PRES uses KL02 and LD06 in the cirrus regime and mixed-phase regime, respectively. Finally, the simulation representing the future period (FUT) has been run with the same model set-up of REF, but it considers the emissions of the RCP6.0 scenario. The comparison between FUT and REF allows us to estimate the changes of the cold cloud (micro)physical processes according to a global warming scenario.



200 4 Results and Discussion

4.1 Global distributions

The global distributions of the vertically integrated tendencies for the REF simulation are shown in Figure 1, and the global means and the standard deviations of the tendencies are shown in Table 3. In cirrus clouds, the largest source of ICs is the instantaneous freezing of supercooled cloud droplets, followed by convective detrainment and then ice nucleation (including
205 homogeneous and heterogeneous nucleation). Both DETR and NCIR are higher over regions that experience strong convective activity, e.g. the Intertropical Convergence Zone (ITCZ) and the Tropical Warm Pool (TWP). DETR is higher over land than over ocean because the land-ocean differences in the thermodynamic profiles below the freezing level produce stronger updrafts over land (Del Genio et al., 2007). Moreover, DETR tends to be smaller off the west coasts of South America, Africa, and Australia where SSTs are colder and stratocumulus decks dominate. FREE shows particularly high values over continents and
210 especially over mountainous regions, where liquid cloud droplets are efficiently transported by strong updrafts up to levels where the temperature is lower than -35°C and freeze. Thus, FREE contributions are high but localised and their annual mean is larger than DETR and NCIR while the FREE annual median is negligible. This is shown in Table 3 (and Subsection 4.3), where the FREE distribution presents the highest variability although its 99th percentile is still negligible. In mixed-phase clouds, the largest IC source is heterogeneous nucleation, followed by secondary ice production, with a distribution (not shown)
215 that is similar to the one of NMIX and whose global mean is lowest among the IC sources (Table 3). NMIX is influenced by the orography (the largest tendencies occur over the Rocky Mountains, the Andes, and the Himalayas) and the abundance of the INPs responsible for heterogeneous nucleation via P13 (i.e. mineral dust, black carbon, soluble organics, and bioaerosols); in fact, high NMIX values are found over the main deserts and downwind areas (e.g. the Saharan region and the Arabian peninsula) and, more generally, in Asia due to high emissions of black carbon and of dust from the Gobi Desert. Globally,
220 $\text{FREE} > \text{DETR} > \text{NCIR} > \text{NMIX} > \text{SECP}$ is the hierarchy of IC sources in REF (Table 3).

Among the IC removal processes (Figure 1), aggregation is the largest IC sink, followed by accretion and sedimentation; self-collection and melting tendencies (not shown) are on average two and four orders of magnitude lower, respectively (Table 3). All sinks show similar patterns, as active aggregation and accretion produce ICs large enough to sediment out, faster than depositional growth. The sink tendencies are higher over land and influenced by the orography. They are also high throughout
225 the mid-latitudes (between 30° and 60°) and over Antarctica, following the vertically integrated ICNC pattern (Figure S1 in the Supplement).

4.2 Annual zonal means

We next explore the zonally averaged profiles of IC sources and sinks in the REF simulation (Figures 2 and 3). We clearly see that ice nucleation in the cirrus regime (NCIR) is the dominant source of ICs in the upper troposphere (at pressures lower
230 than about 350 hPa) and has a maximum in the tropics, coincident with that in ICNC (Figure S2 in the Supplement). In fact, upper-level gravity wave activity, particularly strong in the tropics, can generate temperature fluctuations responsible for strong nucleation tendencies. DETR contributes to produce ICs at temperatures $T < -35^{\circ}\text{C}$ (i.e. in the cirrus regime) especially in



Tendency	REF			PRES			FUT		
	Mean	StDev	99th/1st	Mean	StDev	99th/1st	Mean	StDev	99th/1st
DETR	1.87	53.90	11.14	1.63	50.61	1.51	1.71	46.37	7.97
NCIR	0.52	8.77	10.79	38.71	1734.19	43.48	0.46	5.90	10.00
FREE	77.69	2837.23	0.00	50.55	2267.82	0.00	57.18	2527.37	0.00
NMIX	0.11	3.74	0.80	0.74	42.35	1.42	0.08	3.05	0.57
SECP	0.04	0.67	0.34	0.05	0.68	0.38	0.04	0.62	0.33
SEDI+	3.41	204.92	27.69	3.06	159.89	37.37	2.74	166.00	22.85
MELT	0.00	0.95	0.00	0.00	0.73	0.00	0.00	1.70	0.00
AGGR	-17.59	603.30	-89.16	-14.67	515.83	-131.77	-13.85	560.61	-65.09
ACCR	-9.07	372.28	-38.18	-7.26	318.18	-43.64	-7.06	331.53	-28.20
SELF	-0.10	3.94	-0.36	-0.08	3.29	-0.63	-0.08	3.72	-0.26
SEDI-	-14.75	421.67	-89.23	-12.38	320.19	-162.03	-10.38	357.52	-63.33
Hierarchy (REF and FUT)	Sources: FREE > SEDI+ > DETR > NCIR > NMIX > SECP Sinks: AGGR > SEDI- > ACCR > SELF > MELT								

Table 3. Statistics computed on the 5-hourly ICNC tendencies, output of the simulations REF, PRES, and FUT: global means, standard deviations, 99th/1st percentiles for sources/sinks of ICs (in $\text{m}^{-3}\text{s}^{-1}$). Only the 99th percentiles are shown for the sources as the 1st percentiles are zero; vice versa, only the 1st percentiles are shown for the sinks as the 99th percentiles are zero. Median values are zero for all ICNC tendencies. (Note that SEDI+ and SEDI- take into account only positive and negative values, respectively.) The last two rows summarise the hierarchy of the ICNC tendencies in REF and FUT.

the mid-latitudes (50°N and 50°S), as illustrated in Figure 1. FREE is the highest source of ICs close to the area of transition between cirrus regime and mixed-phase regime and especially outside the tropics. In mixed-phase clouds, NMIX dominates in the mid-latitudes, with values higher in the Northern Hemisphere (NH) than in the Southern Hemisphere (SH) because of higher concentrations of INPs (e.g. Hoose et al., 2010; Liu et al., 2012) and cloud droplets (e.g. Karydis et al., 2017). While NMIX affects the whole mixed-phase regime (i.e. the area between the two isotherms in Figure 2), SECP is more concentrated at lower altitudes, as the Hallett-Mossop process occurs at $-8^{\circ}\text{C} < T < -3^{\circ}\text{C}$. Sedimentation, which is actually a vertical redistribution of ICs, behaves as a source of ICs (i.e. SEDI+) mostly in the mixed-phase regime, where both the number and size of ICs are non-negligible. On the contrary, SEDI+ is low at upper levels because the crystals are too small to fall out and at lower levels because the number of ICs is a small. The global mean of SEDI+ is of the same order of magnitude of DETR, so that the hierarchy of all IC sources is: FREE > SEDI+ > DETR > NCIR > NMIX > SECP (Table 3).

On average, the IC sinks AGGR, ACCR, and SEDI- show similar vertical distributions (Figure 3). Nevertheless, sedimentation is the most significant IC sink in the upper troposphere and in the lower troposphere, extending to higher and lower altitudes than either AGGR or ACCR. Interestingly, the sedimentation-sink (SEDI-) is almost four times larger than the sedimentation-source (SEDI+) (Table 3). While SEDI- involves very many small ICs falling from high latitudes, SEDI+ occurs at lower altitudes where ICs have already undergone growth processes like aggregation that reduce their number. All sink processes but melting show higher values along the transition zone between the two cloud regimes, in particular in the NH and over the Antarctica where ICNCs are higher (Figure S2 in the Supplement). SEDI- and AGGR extend to lower altitudes in the NH than

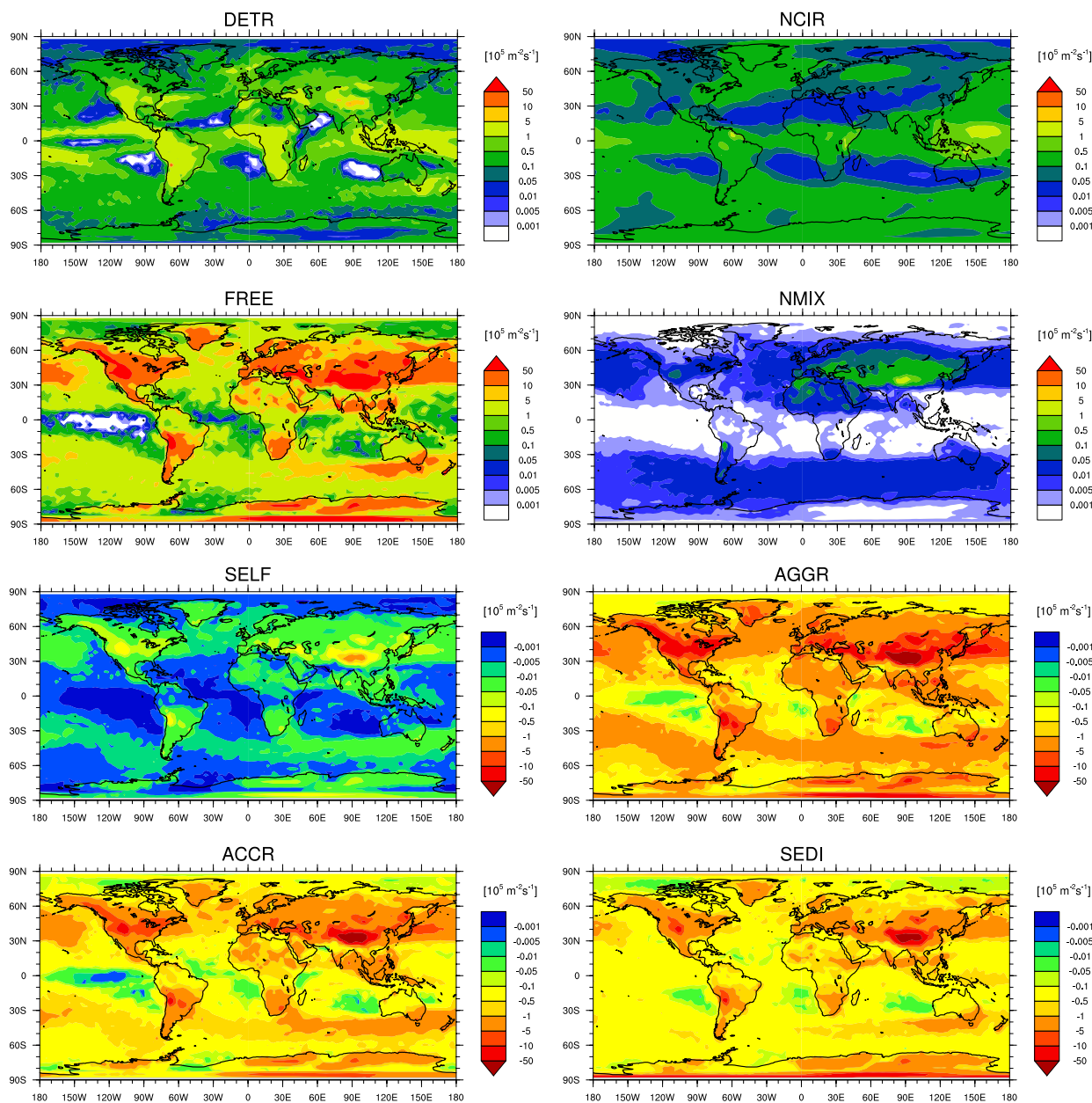


Figure 1. Annual means of the vertically integrated tendencies (in $10^5 \text{ m}^{-2} \text{ s}^{-1}$) for the sources and sinks of ICs in cold clouds (REF simulation).

250 in the SH. Overall, the hierarchy of IC sinks is: $\text{AGGR} > \text{SEDI} > \text{ACCR} > \text{SELF} > \text{MELT}$, where ACCR and SEDI- are of the same order of magnitude (Table 3). It must be noted that IC sources and sinks cannot be expected to balance because the tendency due to advective, turbulent, and convective transport (i.e. R_{transp} in equation (1)) is not computed in the CLOUD

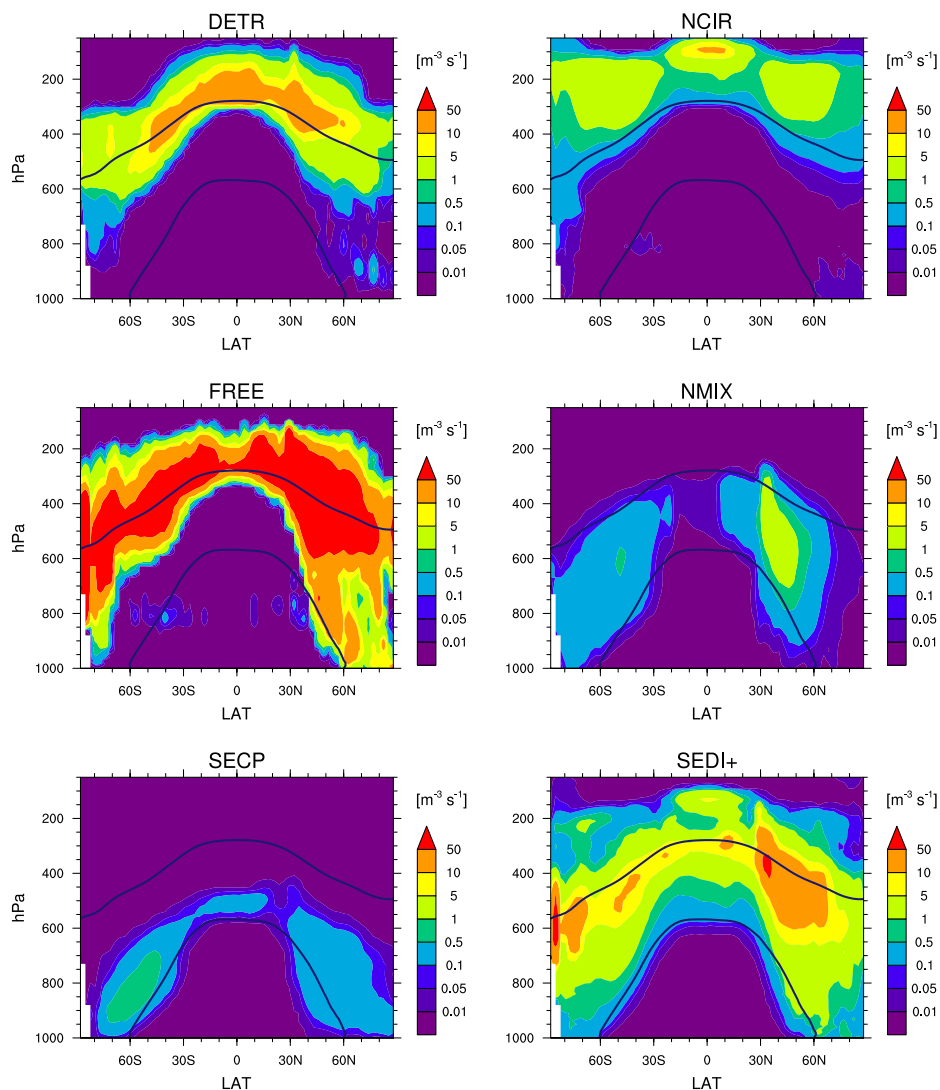


Figure 2. Annual zonal means of the tendencies associated to the IC sources in cold clouds (REF simulation). The isotherms at 0°C and -35°C are annual means. (Note that SEDI here takes into account only positive values.)

submodel but derives from various submodels, e.g. CVTRANS (Tost et al., 2010) and E5VDIFF (Roeckner et al., 2004), and is not shown here.

255 4.3 Regional results

The ICNC tendencies are further analysed at the regional scale. The annual medians of the tendencies are computed in bins of 20 hPa for the following areas (whose coordinates are shown in Figure S1 in the Supplement): Sahara, Amazon, Europe, Atlantic

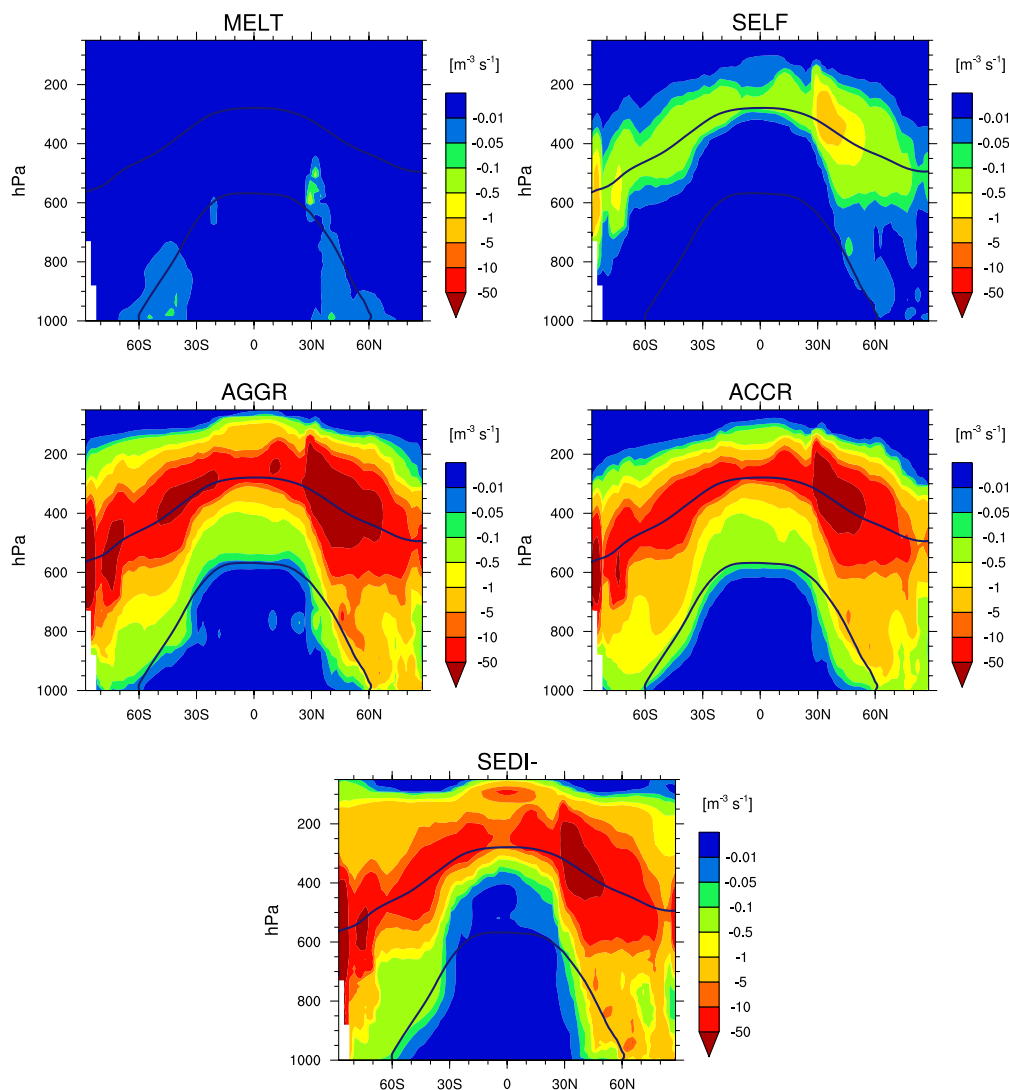


Figure 3. Annual zonal means of the tendencies associated to the IC sinks in cold clouds (REF simulation). The isotherms at 0°C and -35°C are annual means. (Note that SEDI here takes into account only negative values.)

Ocean, and Indian Ocean, and the resulting vertical profiles are shown in Figure 4. In order to appreciate the differences among the microphysical process profiles, only the areas where $\text{ICNC} > 1 \text{ L}^{-1}$ are considered for the computations of the medians, therefore, the tendencies must be compared relative to the ICNC profiles (also shown in Figure 4) as they do not represent absolute values. It appears that ICNC is higher over land than over ocean and the lower the latitude, the higher the altitude associated with the peak in the tendency profiles. Relatively colder surface temperatures over Europe mean both that the European ICNC peak occurs at a lower pressure level and that non-zero tendencies extend down to the surface. It is



interesting that sedimentation shifts from being a sink in the upper troposphere to a source when NCIR tends to zero, in all
265 regions. In the middle and lower troposphere, ICs derive especially from sedimentation and secondary ice production, however,
the contribution to ICNC of ice nucleation in the mixed-phase can be more important in some regions. In fact, NMIX plays
a major role at pressures higher than 600 hPa over the Sahara region because of the new ICs formed heterogeneously from
mineral dust. The regional means (Table S1 in the Supplement) computed for this region indicate that NMIX is more important
than NCIR and SECP, changing the hierarchy found at the global scale. DETR plays a role especially over low latitudes, i.e.
270 over the Sahara and Amazon regions, where strong convective activity is frequent (although over the Amazon only the 75th
percentile is visible while the median is close to zero). On average, DETR is more important than SEDI+ in these regions
(Table S1), thus altering the global hierarchy. AGGR is generally a stronger removal process than ACCR, as mentioned in the
previous section, and its maximum is at higher altitudes than ACCR.

The medians in Figure 4 and the statistics in Table 3 and Table S1 in the Supplement indicate that ICNC tendencies are often
275 characterised by a strong skewed distribution towards high (absolute) values so that their medians and means are very different.
This is valid especially for FREE, with its transitions from being the main source of new ICs in the mean to being a negligible
source in the median.

4.4 Sensitivity studies

4.4.1 Effects due to ice nucleation scheme change

280 Having defined the hierarchy of the ICNC tendencies in REF, we continue with analysing the microphysical processes associ-
ated with different microphysical parameterizations. For this purpose, the ice nucleation parameterizations BN09 and P13 (in
the simulation REF) have been replaced by KL02 and LD06 in the simulation PRES. The comparison of the ICNC tendencies
between REF and PRES is displayed in Figures S3 and S4 in the Supplement. As an expected consequence of the PRES set up,
the ice nucleation tendencies (i.e. NCIR and NMIX) exhibit the strongest differences; both increase, particularly NCIR, whose
285 global mean rises by almost two orders of magnitude. This dramatic increase in NCIR is due to the fact that LD06 parameter-
izes only homogeneous nucleation and disregards the competition for water vapour between homogeneous and heterogeneous
nucleation and the effects of pre-existing ice crystals, producing more, smaller ICs than BN09 (a detailed comparison between
the different ice nucleation parameterizations is given in Bacer et al. (2018)). At the same time, the other processes which
produce new ICs are not associated with significant changes. In fact, DETR, FREE, and SECP results decrease by less than
290 1%, so that their global means are of the same magnitude as those computed in REF (Table 3). As a result, the application of
different parameterizations for ice nucleation has only slightly changed the hierarchy of the IC sources (which now is FREE
> NCIR > SEDI+ > DETR > NMIX > SECP). Among the sinks, SEDI-, SELF, ACCR, and AGGR increase more than 5% in
the upper troposphere (Figure S4). Nevertheless, their overall increase is much smaller than that of NCIR and NMIX. This can
be due to the minor efficiency of these sinks when smaller ICs are involved. (It must be remembered that the change in the
295 transport tendency has not been analysed, thus, sources and sinks cannot be expected to balance.)

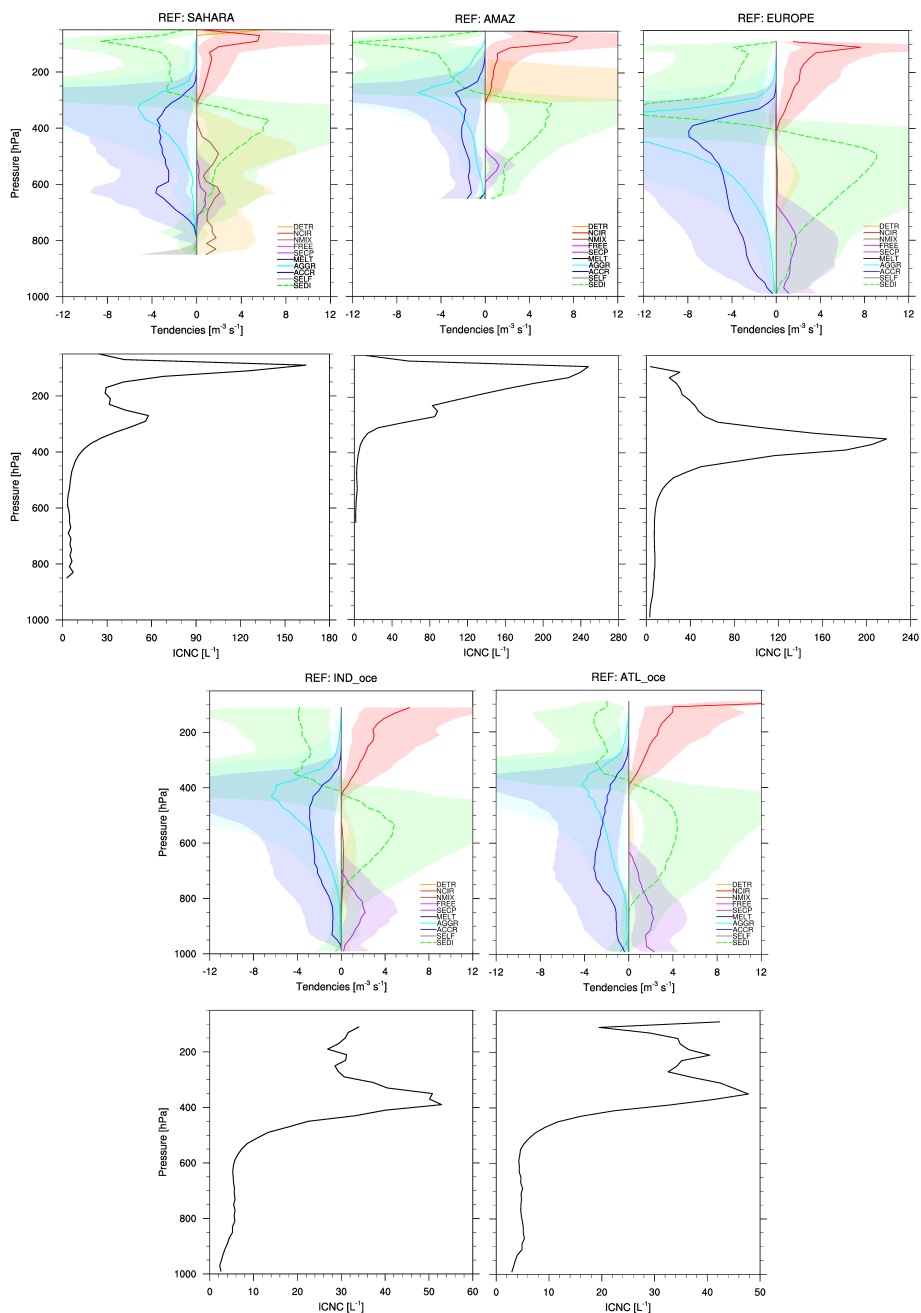


Figure 4. Microphysical process tendencies and ICNC as a function of pressure computed for different regions: Amazon, Sahara, Europe, Indian Ocean, and Atlantic Ocean. The vertical profiles are annual medians computed only where $ICNC > 1 \text{ L}^{-1}$ in bins of 20 hPa. The coloured shadows mark the areas between the 25th and the 75th percentiles.



4.4.2 Effects due to global warming

In order to estimate the global warming effect on cold cloud microphysical processes, the simulations REF and FUT have been compared. The relative percentage changes of the annual zonal means of the FUT tendencies with respect to the REF tendencies are displayed in Figure 5 for the IC sources and Figure S5 in the Supplement for the IC sinks. We found an upward
300 altitude shift of the microphysical processes responsible for both the production and the removal of ICs under a global warming scenario. The reason is that, as the surface temperature warms, the troposphere deepens and the lapse rate becomes less steep; given the cold temperature criteria for most ICNC processes, their contributions must shift upward in altitude to reach the same temperature regime.

All ICNC tendencies increase in intensity (up to 10%) in the upper troposphere, while they slightly decrease (about 1%) at
305 lower altitudes towards the end of the 21st century. This is consistent with the upward shift of the freezing level indicated by the isotherms computed for FUT and in agreement with Del Genio et al. (2007). While SELF, AGGR, and ACCR increase in the “new” cirrus regime, i.e. the area delimited by the isotherm at -35°C computed for FUT, NCIR and DETR mostly increase in the upper troposphere. In particular, DETR increases at the highest levels in the tropics as convection is expected to extend deeper and carry more ICs to these altitudes. However, DETR decreases by a few percent around the -35°C isotherm
310 where the absolute DETR contribution is largest (Figure 2). The decrease of DETR is expected in a warmer climate as an increased upper-tropospheric static stability can reduce the upper-level mass convergence in clear-sky areas, which reduces the convective anvil cloud coverage and in turn the ice detrainment (Bony et al., 2016).

Overall, the ICNC increase in the upper troposphere with respect to recent conditions, as shown in Figure S2 in the Supplement. As a consequence, since the longwave atmospheric heating associated with cirrus clouds is a function of their emissivity
315 and cloud base temperature (Lohmann and Gasparini, 2017), thicker cirrus clouds at higher altitudes enhance atmospheric warming and give rise to a positive feedback in response to surface warming. Moreover, as ICNC increases for a relatively fixed water vapor content in the uppermost atmosphere, the ICs become smaller and their fall speed decrease. A decrease in fall speeds, in turn, translates to more persistent ice clouds that can warm the upper atmosphere over longer times. Indeed, along with the entrainment rate, the IC fall speed has been shown to be a crucial parameter affecting the equilibrium climate
320 sensitivity (i.e. the surface temperature change in response to an increase of carbon dioxide concentration) (Sanderson et al., 2008).

At the global scale, the hierarchy of the ICNC tendencies in FUT remains the same as in REF (Table 3). Moreover, the absolute values of the annual global means computed for FUT are lower than the ones computed for REF, therefore, in the future less new ICs will be produced and more ICs will be removed. In fact, the global average of ICNC decreases in FUT by
325 about 5% with respect to present days.

5 Conclusions

We studied the relative importance of cold cloud microphysical process rates (tendencies) which affect ICNC using global simulations performed with the chemistry-climate model EMAC. The formation processes of ice crystals considered are ice

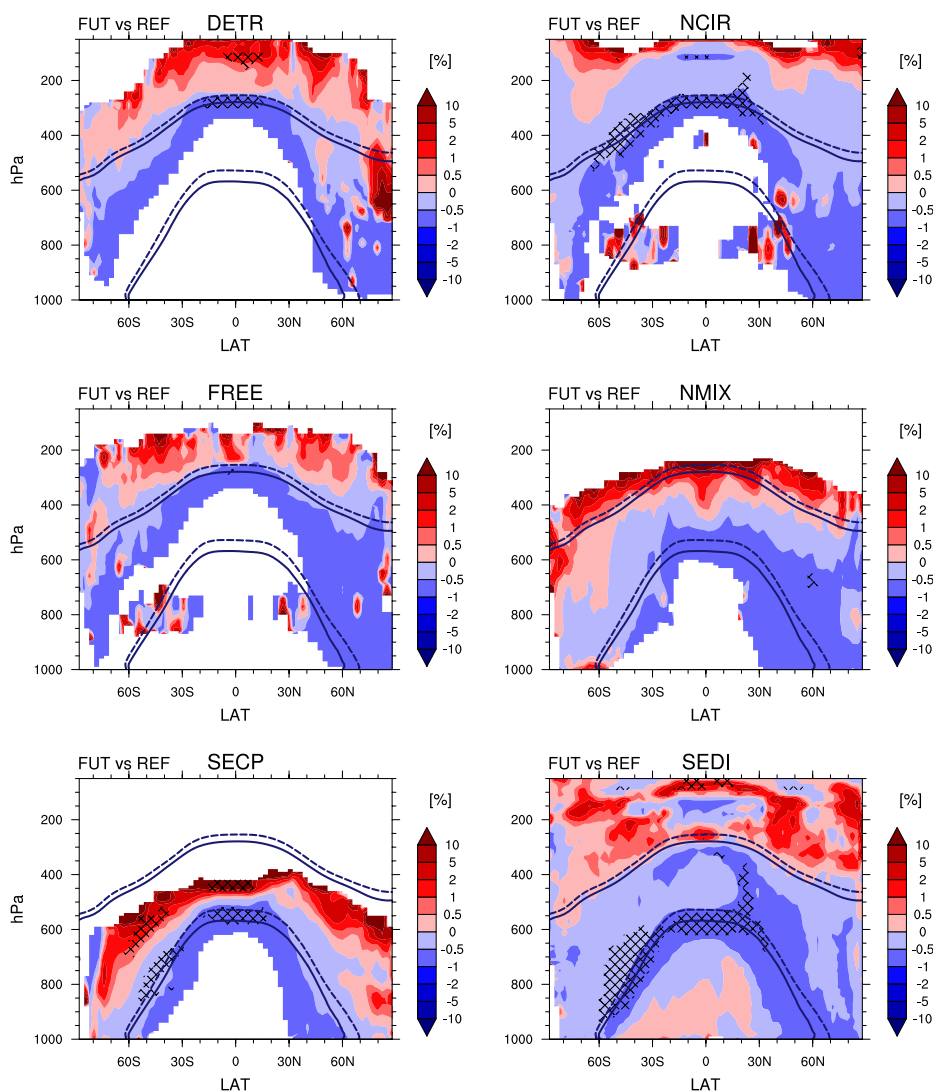


Figure 5. Relative percentage changes of the tendencies associated to the IC sources in cold clouds in FUT with respect to REF, computed where the tendencies in REF are $> 10^{-5} \text{m}^{-3} \text{s}^{-1}$. The hatched pattern indicates areas with a significance level of 70%. The isotherms at 0°C and -35°C are annual means in REF (solid line) and in FUT (dashed line). (Note that SEDI here takes into account only negative values.)

nucleation in the cirrus regime, ice nucleation in the mixed-phase regime, secondary ice production (represented via the Hallett-
330 Mossop process), convective detrainment, and instantaneous freezing of supercooled cloud droplets in liquid-origin cirrus
clouds. The loss processes of ice crystals are melting, self-collection, aggregation, and accretion. Sedimentation was considered
to be a source or sink according to its sign.



We found that orography, dust and anthropogenic particle availability, and land-ocean differences determine much of the spatial variability in the tendency fields. We defined the hierarchy of sources and sinks of ice crystals at the global scale.
335 We found that, on average, the hierarchy of the IC sources is FREE > SEDI+ > DETR > NCIR > NMIX > SECP, while the hierarchy of the IC sinks is AGGR > SEDI- > ACCR > SELF > MELT.

Regionally, the relative importance of the microphysical processes can be different. For example, convective detrainment is more important than sedimentation over the Sahara and Amazon (regions at low latitudes), while heterogeneous nucleation in the mixed-phase regime is slightly more important than NCIR over the Sahara, because of the role of mineral dust as INP.
340 ICNCs peak at lower altitudes over the oceans and mid-latitude regions than over the tropical land masses, as do their accretion and aggregation sinks and sedimentation sources.

The distributions of the tendencies are strongly asymmetric with most of them being close to zero and large tails (as shown by the 1st and 99th percentiles computed for sinks and sources, respectively). The asymmetry persists even when tendencies are computed in volumes of air where $ICNC > 1 L^{-1}$, although the skewness is less marked in this case (not shown).

345 Additionally, we found that the application of different parameterizations for ice nucleation changed the ice nucleation tendencies but affected only slightly the hierarchy of the IC sources. The large variation in ICNC output from these nucleation parameterizations highlights the importance of including the competition for water vapor between INPs and pre-existing ice crystals (Bacer et al., 2018). We also computed the tendencies in a future climate (using the RCP6.0 scenario). Our results showed an upward shift of the freezing level and the associated microphysical processes to higher altitudes, consistent with a
350 reduced lapse rate that is expected to accompany surface temperature warming. The tendencies increase in the cirrus regime (NCIR and DETR especially in the upper troposphere) where their radiative effect is largest; however, they are found to undergo an overall reduction at the global scale.

Knowing the relative importance of the microphysical process rates is of fundamental importance to assign priority to the development of microphysics parameterizations. Moreover, the quantification of tendencies is essential to compare model
355 output and observations which have different temporal resolutions. In future studies of the relative importance of the cold cloud microphysical processes it would be useful to perform a similar analyses for the mass tendencies, i.e. the rates of cloud ice mixing ratios. Moreover, the transport tendencies could be included.

Data availability. The simulation data used in this study are available upon request.

Author contributions. SB performed the model simulations and carried out the analysis, which was planned with SS, AP, and HT. SB
360 prepared the manuscript, together with SS. All the authors provided assistance in finalizing the analysis and the manuscript.

Competing interests. The authors declare that they have no conflict of interest.



Acknowledgements. We would like to thank Sergey Gromov from the Max Planck Institute for Chemistry for the discussion on the model results. SS was funded by the DFG project TropiC in collaboration with NSF PIRE project 1743753. HT acknowledges funding from the Carl-Zeiss foundation. We acknowledge the usage of the Max Planck Computing and Data Facility (MPCDF) for the simulations performed in this work.

365



References

- Bacer, S., Sullivan, S. C., Karydis, V. A., Barahona, D., Krämer, M., Nenes, A., Tost, H., Tsimpidi, A. P., Lelieveld, J., and Pozzer, A.: Implementation of a comprehensive ice crystal formation parameterization for cirrus and mixed-phase clouds in the EMAC model (based on MESSy 2.53), *Geoscientific Model Development*, 11, 4021–4041, <https://doi.org/10.5194/gmd-11-4021-2018>, <https://www.geosci-model-dev.net/11/4021/2018/>, 2018.
- 370
- Barahona, D. and Nenes, A.: Parameterization of cirrus cloud formation in large-scale models: Homogeneous nucleation, *Journal of Geophysical Research: Atmospheres*, 113, n/a–n/a, <https://doi.org/10.1029/2007JD009355>, d11211, 2008.
- Barahona, D. and Nenes, A.: Parameterizing the competition between homogeneous and heterogeneous freezing in ice cloud formation - polydisperse ice nuclei, *Atmospheric Chemistry and Physics*, 9, 5933–5948, <https://doi.org/10.5194/acp-9-5933-2009>, <https://www.atmos-chem-phys.net/9/5933/2009/>, 2009.
- 375
- Barahona, D., Molod, A., Bacmeister, J., Nenes, A., Gettelman, A., Morrison, H., Phillips, V., and Eichmann, A.: Development of two-moment cloud microphysics for liquid and ice within the NASA Goddard Earth Observing System Model (GEOS-5), *Geoscientific Model Development*, 7, 1733–1766, <https://doi.org/10.5194/gmd-7-1733-2014>, <https://www.geosci-model-dev.net/7/1733/2014/>, 2014.
- Bony, S., Stevens, B., Coppin, D., Becker, T., Reed, K. A., Voigt, A., and Medeiros, B.: Thermodynamic control of anvil cloud amount, *Proceedings of the National Academy of Sciences*, 113, 8927–8932, <https://doi.org/10.1073/pnas.1601472113>, <https://www.pnas.org/content/113/32/8927>, 2016.
- 380
- Brinkop, S. and Roeckner, E.: Sensitivity of a general circulation model to parameterizations of cloud–turbulence interactions in the atmospheric boundary layer, *Tellus A*, 47, 197–220, <https://doi.org/10.1034/j.1600-0870.1995.t01-1-00004.x>, 1995.
- Cantrell, W. and Heymsfield, A.: Production of Ice in Tropospheric Clouds: A Review, *Bulletin of the American Meteorological Society*, 86, 795–807, <https://doi.org/10.1175/BAMS-86-6-795>, 2005.
- 385
- Chen, T., Rossow, W. B., and Zhang, Y.: Radiative Effects of Cloud-Type Variations, *Journal of Climate*, 13, 264–286, [https://doi.org/10.1175/1520-0442\(2000\)013<0264:REOCTV>2.0.CO;2](https://doi.org/10.1175/1520-0442(2000)013<0264:REOCTV>2.0.CO;2), 2000.
- Collins, W. J., Bellouin, N., Doutriaux-Boucher, M., Gedney, N., Halloran, P., Hinton, T., Hughes, J., Jones, C. D., Joshi, M., Liddicoat, S., Martin, G., O'Connor, F., Rae, J., Senior, C., Sitch, S., Totterdell, I., Wiltshire, A., and Woodward, S.: Development and evaluation of an Earth-System model – HadGEM2, *Geosci. Model Dev.*, 4, 1051–1075, <https://doi.org/10.5194/gmd-4-1051-2011>, 2011.
- 390
- Del Genio, A. D., Yao, M.-S., and Jonas, J.: Will moist convection be stronger in a warmer climate?, *Geophysical Research Letters*, 34, <https://doi.org/10.1029/2007GL030525>, <https://agupubs.onlinelibrary.wiley.com/doi/abs/10.1029/2007GL030525>, 2007.
- DeMott, P. J., Prenni, A. J., Liu, X., Kreidenweis, S. M., Petters, M. D., Twohy, C. H., Richardson, M. S., Eidhammer, T., and Rogers, D. C.: Predicting global atmospheric ice nuclei distributions and their impacts on climate, *Proceedings of the National Academy of Sciences*, 107, 11 217–11 222, <https://doi.org/10.1073/pnas.0910818107>, 2010.
- 395
- DeMott, P. J., Hill, T. C. J., McCluskey, C. S., Prather, K. A., Collins, D. B., Sullivan, R. C., Ruppel, M. J., Mason, R. H., Irish, V. E., Lee, T., Hwang, C. Y., Rhee, T. S., Snider, J. R., McMeeking, G. R., Dhaniyala, S., Lewis, E. R., Wentzell, J. J. B., Abbatt, J., Lee, C., Sultana, C. M., Ault, A. P., Axson, J. L., Diaz Martinez, M., Venero, I., Santos-Figueroa, G., Stokes, M. D., Deane, G. B., Mayol-Bracero, O. L., Grassian, V. H., Bertram, T. H., Bertram, A. K., Moffett, B. F., and Franc, G. D.: Sea spray aerosol as a unique source of ice nucleating particles, *Proceedings of the National Academy of Sciences*, 113, 5797–5803, <https://doi.org/10.1073/pnas.1514034112>, <http://www.pnas.org/content/113/21/5797.abstract>, 2016.
- 400



- Dietmüller, S., Jöckel, P., Tost, H., Kunze, M., Gellhorn, C., Brinkop, S., Frömming, C., Ponater, M., Steil, B., Lauer, A., and Hendricks, J.: A new radiation infrastructure for the Modular Earth Submodel System (MESSy, based on version 2.51), *Geoscientific Model Development*, 9, 2209–2222, <https://doi.org/10.5194/gmd-9-2209-2016>, <https://www.geosci-model-dev.net/9/2209/2016/>, 2016.
- 405 Fujino, J., Nair, R., Kainuma, M., Masui, T., and Matsuoka, Y.: Multi-gas Mitigation Analysis on Stabilization Scenarios Using Aim Global Model, *The Energy Journal*, 3, 343–354, 2006.
- Gottelman, A., Morrison, H., Terai, C. R., and Wood, R.: Microphysical process rates and global aerosol–cloud interactions, *Atmospheric Chemistry and Physics*, 13, 9855–9867, <https://doi.org/10.5194/acp-13-9855-2013>, <https://www.atmos-chem-phys.net/13/9855/2013/>, 2013.
- 410 Guo, H., Liu, Y., Daum, P. H., Senum, G. I., and Tao, W.-K.: Characteristics of vertical velocity in marine stratocumulus: comparison of large eddy simulations with observations, *Environmental Research Letters*, 3, 1–8, <https://doi.org/10.1088/1748-9326/3/4/045020>, 2008.
- Hallett, J. and Mossop, S. C.: Production of secondary ice particles during the riming process, *Nature*, 249, 26–28, <https://doi.org/10.1038/249026a0>, 1974.
- Heymsfield, A. J., Krämer, M., Luebke, A., Brown, P., Cziczo, D. J., Franklin, C., Lawson, P., Lohmann, U., McFarquhar, G., Ulanowski, Z., and Van Tricht, K.: Cirrus Clouds, *Meteorological Monographs*, 58, 2.1–2.26, <https://doi.org/10.1175/AMSMONOGRAPHS-D-16-0010.1>, 2017.
- Hong, Y., Liu, G., and Li, J.-L. F.: Assessing the Radiative Effects of Global Ice Clouds Based on CloudSat and CALIPSO Measurements, *Journal of Climate*, 29, 7651–7674, <https://doi.org/10.1175/JCLI-D-15-0799.1>, 2016.
- Hoose, C., Kristjánsson, J. E., and Burrows, S. M.: How important is biological ice nucleation in clouds on a global scale?, *Environmental Research Letters*, 5, 024 009, <http://stacks.iop.org/1748-9326/5/i=2/a=024009>, 2010.
- IPCC: *Climate Change 2013: The Physical Science Basis*, Cambridge University Press, 1535 pp., 2013.
- Jensen, E. J., Diskin, G., Lawson, R. P., Lance, S., Bui, T. P., Hlavka, D., McGill, M., Pfister, L., Toon, O. B., and Gao, R.: Ice nucleation and dehydration in the Tropical Tropopause Layer, *Proceedings of the National Academy of Sciences*, 110, 2041–2046, <https://doi.org/10.1073/pnas.1217104110>, <http://www.pnas.org/content/110/6/2041>, 2013.
- 425 Jöckel, P., Kerkweg, A., Pozzer, A., Sander, R., Tost, H., Riede, H., Baumgaertner, A., Gromov, S., and Kern, B.: Development cycle 2 of the Modular Earth Submodel System (MESSy2), *Geoscientific Model Development*, 3, 717–752, <https://doi.org/10.5194/gmd-3-717-2010>, <https://www.geosci-model-dev.net/3/717/2010/>, 2010.
- Jöckel, P., Tost, H., Pozzer, A., Kunze, M., Kirner, O., Brenninkmeijer, C. A. M., Brinkop, S., Cai, D. S., Dyroff, C., Eckstein, J., Frank, F., Garny, H., Gottschaldt, K.-D., Graf, P., Grewe, V., Kerkweg, A., Kern, B., Matthes, S., Mertens, M., Meul, S., Neumaier, M., Nützel, M., Oberländer-Hayn, S., Ruhnke, R., Runde, T., Sander, R., Scharffe, D., and Zahn, A.: Earth System Chemistry integrated Modelling (ESCiMo) with the Modular Earth Submodel System (MESSy) version 2.51, *Geoscientific Model Development*, 9, 1153–1200, <https://doi.org/10.5194/gmd-9-1153-2016>, <https://www.geosci-model-dev.net/9/1153/2016/>, 2016.
- 430 Kanji, Z. A., Ladino, L. A., Wex, H., Boose, Y., Burkert-Kohn, M., Cziczo, D. J., and Krämer, M.: Overview of Ice Nucleating Particles, *Meteorological Monographs*, 58, 1.1–1.33, <https://doi.org/10.1175/AMSMONOGRAPHS-D-16-0006.1>, 2017.
- 435 Kärcher, B. and Lohmann, U.: A parameterization of cirrus cloud formation: Homogeneous freezing of supercooled aerosols, *Journal of Geophysical Research: Atmospheres*, 107, AAC 4–1–AAC 4–10, <https://doi.org/10.1029/2001JD000470>, 2002a.
- Kärcher, B. and Lohmann, U.: A Parameterization of cirrus cloud formation: Homogeneous freezing including effects of aerosol size, *Journal of Geophysical Research: Atmospheres*, 107, AAC 9–1–AAC 9–10, <https://doi.org/10.1029/2001JD001429>, 2002b.



- 440 Karydis, V. A., Kumar, P., Barahona, D., Sokolik, I. N., and Nenes, A.: On the effect of dust particles on global cloud condensation nuclei and cloud droplet number, *Journal of Geophysical Research: Atmospheres*, 116, <https://doi.org/10.1029/2011JD016283>, d23204, 2011.
- Karydis, V. A., Tsimpidi, A. P., Pozzer, A., Astitha, M., and Lelieveld, J.: Effects of mineral dust on global atmospheric nitrate concentrations, *Atmospheric Chemistry and Physics*, 16, 1491–1509, <https://doi.org/10.5194/acp-16-1491-2016>, <https://www.atmos-chem-phys.net/16/1491/2016/>, 2016.
- 445 Karydis, V. A., Tsimpidi, A. P., Bacer, S., Pozzer, A., Nenes, A., and Lelieveld, J.: Global impact of mineral dust on cloud droplet number concentration, *Atmospheric Chemistry and Physics*, 17, 5601–5621, <https://doi.org/10.5194/acp-17-5601-2017>, <https://www.atmos-chem-phys.net/17/5601/2017/>, 2017.
- Kerkweg, A., Buchholz, J., Ganzeveld, L., Pozzer, A., Tost, H., and Jöckel, P.: Technical Note: An implementation of the dry removal processes DRY DEPosition and SEDimentation in the Modular Earth Submodel System (MESSy), *Atmospheric Chemistry and Physics*, 6, 4617–4632, <https://doi.org/10.5194/acp-6-4617-2006>, <https://www.atmos-chem-phys.net/6/4617/2006/>, 2006a.
- 450 Kerkweg, A., Sander, R., Tost, H., and Jöckel, P.: Technical note: Implementation of prescribed (OFFLEM), calculated (ONLEM), and pseudo-emissions (TNUDGE) of chemical species in the Modular Earth Submodel System (MESSy), *Atmospheric Chemistry and Physics*, 6, 3603–3609, <https://doi.org/10.5194/acp-6-3603-2006>, <https://www.atmos-chem-phys.net/6/3603/2006/>, 2006b.
- Khain, A. P. and Pinsky, M.: *Physical processes in clouds and in cloud modeling*, Cambridge University Press, 2018.
- 455 Klingmüller, K., Metzger, S., Abdelkader, M., Karydis, V. A., Stenchikov, G. L., Pozzer, A., and Lelieveld, J.: Revised mineral dust emissions in the atmospheric chemistry-climate model EMAC (MESSy 2.52 DU_Astitha1KKDU2017 patch), *Geoscientific Model Development Discussions*, 11, 989–1008, <https://doi.org/10.5194/gmd-11-989-2018>, 2018.
- Korolev, A., McFarquhar, G., Field, P. R., Franklin, C., Lawson, P., Wang, Z., Williams, E., Abel, S. J., Axisa, D., Borrmann, S., Crosier, J., Fugal, J., Krämer, M., Lohmann, U., Schlenker, O., Schnaiter, M., and Wendisch, M.: *Mixed-Phase Clouds: Progress and Challenges*, *Meteorological Monographs*, 58, 5.1–5.50, <https://doi.org/10.1175/AMSMONOGRAPHS-D-17-0001.1>, 2017.
- 460 Krämer, M., Rolf, C., Luebke, A., Afchine, A., Spelten, N., Costa, A., Meyer, J., Zöger, M., Smith, J., Herman, R. L., Buchholz, B., Ebert, V., Baumgardner, D., Borrmann, S., Klingebiel, M., and Avallone, L.: A microphysics guide to cirrus clouds – Part I: Cirrus types, *Atmospheric Chemistry and Physics*, 16, 3463–3483, <https://doi.org/10.5194/acp-16-3463-2016>, <https://www.atmos-chem-phys.net/16/3463/2016/>, 2016.
- 465 Kuebbeler, M., Lohmann, U., Hendricks, J., and Kärcher, B.: Dust ice nuclei effects on cirrus clouds, *Atmospheric Chemistry and Physics*, 14, 3027–3046, <https://doi.org/10.5194/acp-14-3027-2014>, <https://www.atmos-chem-phys.net/14/3027/2014/>, 2014.
- Kumar, P., Sokolik, I. N., and Nenes, A.: Parameterization of cloud droplet formation for global and regional models: including adsorption activation from insoluble CCN, *Atmospheric Chemistry and Physics*, 9, 2517–2532, <https://doi.org/10.5194/acp-9-2517-2009>, <https://www.atmos-chem-phys.net/9/2517/2009/>, 2009.
- 470 Kumar, P., Sokolik, I. N., and Nenes, A.: Cloud condensation nuclei activity and droplet activation kinetics of wet processed regional dust samples and minerals, *Atmospheric Chemistry and Physics*, 11, 8661–8676, <https://doi.org/10.5194/acp-11-8661-2011>, <https://www.atmos-chem-phys.net/11/8661/2011/>, 2011.
- 475 Lamarque, J.-F., Bond, T. C., Eyring, V., Granier, C., Heil, A., Klimont, Z., Lee, D., Liousse, C., Mieville, A., Owen, B., Schultz, M. G., Shindell, D., Smith, S. J., Stehfest, E., Van Aardenne, J., Cooper, O. R., Kainuma, M., Mahowald, N., McConnell, J. R., Naik, V., Riahi, K., and van Vuuren, D. P.: Historical (1850–2000) gridded anthropogenic and biomass burning emissions of reactive gases and aerosols: methodology and application, *Atmospheric Chemistry and Physics*, 10, 7017–7039, <https://doi.org/10.5194/acp-10-7017-2010>, <https://www.atmos-chem-phys.net/10/7017/2010/>, 2010.



- Lawson, R. P., Woods, S., Jensen, E., Erfani, E., Gurganus, C., Gallagher, M., Connolly, P., Whiteway, J., Baran, A. J., May, P., Heymsfield, A., Schmitt, C. G., McFarquhar, G., Um, J., Protat, A., Bailey, M., Lance, S., Muehlbauer, A., Stith, J., Korolev, A., Toon, O. B., and Krämer, M.: A Review of Ice Particle Shapes in Cirrus formed In Situ and in Anvils, *Journal of Geophysical Research: Atmospheres*, 124, 10 049–10 090, <https://doi.org/10.1029/2018JD030122>, <https://agupubs.onlinelibrary.wiley.com/doi/abs/10.1029/2018JD030122>, 2019.
- 480 Levkov, L., Rockel, B., Kapitzka, H., and E., R.: 3D mesoscale numerical studies of cirrus and stratus clouds by their time and space evolution, *Beitr. Phys. Atmos.*, 65, 35–58, 1992.
- Lin, Y.-L., Farley, R. D., and Orville, H. D.: Bulk Parameterization of the Snow Field in a Cloud Model, *Journal of Climate and Applied Meteorology*, 22, 1065–1092, [https://doi.org/10.1175/1520-0450\(1983\)022<1065:BPOTSF>2.0.CO;2](https://doi.org/10.1175/1520-0450(1983)022<1065:BPOTSF>2.0.CO;2), 1983.
- 485 Liu, X., Shi, X., Zhang, K., Jensen, E. J., Gettelman, A., Barahona, D., Nenes, A., and Lawson, P.: Sensitivity studies of dust ice nuclei effect on cirrus clouds with the Community Atmosphere Model CAM5, *Atmospheric Chemistry and Physics*, 12, 12 061–12 079, <https://doi.org/10.5194/acp-12-12061-2012>, <https://www.atmos-chem-phys.net/12/12061/2012/>, 2012.
- Lohmann, U.: Possible Aerosol Effects on Ice Clouds via Contact Nucleation, *Journal of the Atmospheric Sciences*, 59, 647–656, [https://doi.org/10.1175/1520-0469\(2001\)059<0647:PAEOIC>2.0.CO;2](https://doi.org/10.1175/1520-0469(2001)059<0647:PAEOIC>2.0.CO;2), 2002.
- 490 Lohmann, U. and Diehl, K.: Sensitivity Studies of the Importance of Dust Ice Nuclei for the Indirect Aerosol Effect on Stratiform Mixed-Phase Clouds, *Journal of the Atmospheric Sciences*, 63, 968–982, <https://doi.org/10.1175/JAS3662.1>, 2006.
- Lohmann, U. and Gasparini, B.: A cirrus cloud climate dial?, *Science*, 357, 248–249, <https://doi.org/10.1126/science.aan3325>, <https://science.sciencemag.org/content/357/6348/248>, 2017.
- Lohmann, U. and Kärcher, B.: First interactive simulations of cirrus clouds formed by homogeneous freezing in the ECHAM general circulation model, *Journal of Geophysical Research: Atmospheres*, 107, AAC 8–1–AAC 8–13, <https://doi.org/10.1029/2001JD000767>, 2002.
- 495 Lohmann, U., Feichter, J., Chuang, C. C., and Penner, J. E.: Prediction of the number of cloud droplets in the ECHAM GCM, *Journal of Geophysical Research: Atmospheres*, 104, 9169–9198, <https://doi.org/10.1029/1999JD900046>, 1999.
- Lohmann, U., Stier, P., Hoose, C., Ferrachat, S., Kloster, S., Roeckner, E., and Zhang, J.: Cloud microphysics and aerosol indirect effects in the global climate model ECHAM5-HAM, *Atmospheric Chemistry and Physics*, 7, 3425–3446, <https://doi.org/10.5194/acp-7-3425-2007>, <https://www.atmos-chem-phys.net/7/3425/2007/>, 2007.
- 500 Matus, A. V. and L'Ecuyer, T. S.: The role of cloud phase in Earth's radiation budget, *Journal of Geophysical Research: Atmospheres*, 122, 2559–2578, <https://doi.org/10.1002/2016JD025951>, 2017.
- Nordeng, T. E.: Extended versions of the convection parametrization scheme at ECMWF and their impact upon the mean climate and transient activity of the model in the tropics, *ECMWF Tech. Memo. No. 206*, 1994.
- 505 Petters, M. D. and Kreidenweis, S. M.: A single parameter representation of hygroscopic growth and cloud condensation nucleus activity, *Atmospheric Chemistry and Physics*, 7, 1961–1971, <https://doi.org/10.5194/acp-7-1961-2007>, <https://www.atmos-chem-phys.net/7/1961/2007/>, 2007.
- Phillips, V. T. J., Donner, L. J., and Garner, S. T.: Nucleation Processes in Deep Convection Simulated by a Cloud-System-Resolving Model with Double-Moment Bulk Microphysics, *Journal of the Atmospheric Sciences*, 64, 738–761, <https://doi.org/10.1175/JAS3869.1>, 2007.
- 510 Phillips, V. T. J., Demott, P. J., Andronache, C., Pratt, K. A., Prather, K. A., Subramanian, R., and Twohy, C.: Improvements to an Empirical Parameterization of Heterogeneous Ice Nucleation and Its Comparison with Observations, *Journal of the Atmospheric Sciences*, 70, 378–409, <https://doi.org/10.1175/JAS-D-12-080.1>, 2013.



- Pozzer, A., de Meij, A., Pringle, K. J., Tost, H., Doering, U. M., van Aardenne, J., and Lelieveld, J.: Distributions and regional budgets of aerosols and their precursors simulated with the EMAC chemistry-climate model, *Atmospheric Chemistry and Physics*, 12, 961–987, <https://doi.org/10.5194/acp-12-961-2012>, <https://www.atmos-chem-phys.net/12/961/2012/>, 2012.
- Pozzer, A., de Meij, A., Yoon, J., Tost, H., Georgoulias, A. K., and Astitha, M.: AOD trends during 2001–2010 from observations and model simulations, *Atmospheric Chemistry and Physics*, 15, 5521–5535, <https://doi.org/10.5194/acp-15-5521-2015>, <https://www.atmos-chem-phys.net/15/5521/2015/>, 2015.
- Pringle, K. J., Tost, H., Message, S., Steil, B., Giannadaki, D., Nenes, A., Fountoukis, C., Stier, P., Vignati, E., and Lelieveld, J.: Description and evaluation of GMXe: a new aerosol submodel for global simulations (v1), *Geoscientific Model Development*, 3, 391–412, <https://doi.org/10.5194/gmd-3-391-2010>, <https://www.geosci-model-dev.net/3/391/2010/>, 2010.
- Pruppacher, H. R. and Klett, J. D.: *Microphysics of Clouds and Precipitation*, Springer, New York, 954 pp, 1997.
- Roeckner, E., Brokopf, R., Esch, M., Giorgetta, M., Hagemann, S., Kornbluh, L., Schlese, U., Schulzweida, U., and Manzini, E.: The Atmospheric General Circulation Model ECHAM5, Part II, *Max-Planck-Institut für Meteorologie*, p. 25, 2004.
- Roeckner, E., Brokopf, R., Esch, M., Giorgetta, M., Hagemann, S., Kornbluh, L., Manzini, E., Schlese, U., and Schulzweida, U.: Sensitivity of Simulated Climate to Horizontal and Vertical Resolution in the ECHAM5 Atmosphere Model, *Journal of Climate*, 19, 3771–3791, <https://doi.org/10.1175/JCLI3824.1>, 2006.
- Rogers, R. R. and Yau, M. K.: *A short course in cloud physics*, Butterworth-Heinemann, 3rd edn., 1989.
- Sander, R., Baumgaertner, A., Gromov, S., Harder, H., Jöckel, P., Kerkweg, A., Kubistin, D., Regelin, E., Riede, H., Sandu, A., Taraborrelli, D., Tost, H., and Xie, Z.-Q.: The atmospheric chemistry box model CAABA/MECCA-3.0, *Geoscientific Model Development*, 4, 373–380, <https://doi.org/10.5194/gmd-4-373-2011>, <https://www.geosci-model-dev.net/4/373/2011/>, 2011.
- Sanderson, B. M., Piani, C., Ingram, W. J., A., S. D., and R., A. M.: Towards constraining climate sensitivity by linear analysis of feedback patterns in thousands of perturbed-physics GCM simulations, *Climate Dynamics*, 30, 175–190, <https://doi.org/10.1007/s00382-007-0280-7>, 2008.
- Seinfeld, J. H., Bretherton, C., Carslaw, K. S., Coe, H., DeMott, P. J., Dunlea, E. J., Feingold, G., Ghan, S., Guenther, A. B., Kahn, R., Kraucunas, I., Kreidenweis, S. M., Molina, M. J., Nenes, A., Penner, J. E., Prather, K. A., Ramanathan, V., Ramaswamy, V., Rasch, P. J., Ravishankara, A. R., Rosenfeld, D., Stephens, G., and Wood, R.: Improving our fundamental understanding of the role of aerosol-cloud interactions in the climate system, *Proceedings of the National Academy of Sciences*, 113, 5781–5790, <https://doi.org/10.1073/pnas.1514043113>, <http://www.pnas.org/content/113/21/5781>, 2016.
- Sullivan, S. C., Barthlott, C., Crosier, J., Zhukov, I., Nenes, A., and Hoose, C.: The effect of secondary ice production parameterization on the simulation of a cold frontal rainband, *Atmospheric Chemistry and Physics*, 18, 16 461–16 480, <https://doi.org/10.5194/acp-18-16461-2018>, <https://www.atmos-chem-phys.net/18/16461/2018/>, 2018a.
- Sullivan, S. C., Hoose, C., Kiselev, A., Leisner, T., and Nenes, A.: Initiation of secondary ice production in clouds, *Atmospheric Chemistry and Physics*, 18, 1593–1610, <https://doi.org/10.5194/acp-18-1593-2018>, <https://www.atmos-chem-phys.net/18/1593/2018/>, 2018b.
- Sundqvist, H., Berge, E., and Kristjansson, J. E.: Condensation and Cloud Parameterization Studies with a Mesoscale NUmberical Weather Prediction Model, *Monthly Weather Review*, 117, 1641–1657, 1989.
- Tiedtke, M.: A Comprehensive Mass Flux Scheme for Cumulus Parameterization in Large-Scale Models, *Monthly Weather Review*, 117, 1779–1800, [https://doi.org/10.1175/1520-0493\(1989\)117<1779:ACMFSF>2.0.CO;2](https://doi.org/10.1175/1520-0493(1989)117<1779:ACMFSF>2.0.CO;2), 1989.



- 550 Tost, H., Jöckel, P., Kerkweg, A., Sander, R., and Lelieveld, J.: Technical note: A new comprehensive SCAVenging submodel for global atmospheric chemistry modelling, *Atmospheric Chemistry and Physics*, 6, 565–574, <https://doi.org/10.5194/acp-6-565-2006>, <https://www.atmos-chem-phys.net/6/565/2006/>, 2006a.
- Tost, H., Jöckel, P., and Lelieveld, J.: Influence of different convection parameterisations in a GCM, *Atmospheric Chemistry and Physics*, 6, 5475–5493, <https://doi.org/10.5194/acp-6-5475-2006>, <https://www.atmos-chem-phys.net/6/5475/2006/>, 2006b.
- 555 Tost, H., Lawrence, M. G., Brühl, C., Jöckel, P., Team, T. G., and Team, T. S.-O.-D.: Uncertainties in atmospheric chemistry modelling due to convection parameterisations and subsequent scavenging, *Atmospheric Chemistry and Physics*, 10, 1931–1951, <https://doi.org/10.5194/acp-10-1931-2010>, <https://www.atmos-chem-phys.net/10/1931/2010/>, 2010.
- Tsimpidi, A. P., Karydis, V. A., Pandis, S. N., and Lelieveld, J.: Global combustion sources of organic aerosols: model comparison with 84 AMS factor-analysis data sets, *Atmospheric Chemistry and Physics*, 16, 8939–8962, <https://doi.org/10.5194/acp-16-8939-2016>, <https://www.atmos-chem-phys.net/16/8939/2016/>, 2016.